

Journal of the Algerian Chemical Society

Journal homepage: https://www.jacs-dz.org

ISSN 1111-4797



COMPUTATIONAL ANALYSIS OF N-FERROCENYLMETHYL-N-PHENYLBENZOHYDRAZIDE: MOLECULAR DOCKING AND DYNAMIC STABILITY WITH BSA

Yahia Bekkar¹*, Zahra Saada^{1,2}, Aida Benine¹

¹VTRS Laboratory, Faculty of exact Sciences, University of El Oued, 39000, El Oued, Algeria ²VPRS Laboratory, Faculty of Mathematics and Matter Sciences, University of Ouargla. 30000, Ouargla, Algeria

ABSTRACT

Article History

Received: 17/12/2024

Revised: 28/12/2024

Accepted: 29/12/2024

This study provides a comprehensive computational analysis of N-ferrocenylmethyl-N-phenylbenzohydrazide (FHD) as a potential bioactive compound by employing density functional theory (DFT), molecular docking, and molecular dynamics (MD) simulations. DFT calculations, including frontier molecular orbital and molecular electrostatic potential analyses, reveal the electronic structure and reactive regions of FHD. Reduced density gradient analysis highlights weak intermolecular interactions, confirming molecular stability. Molecular docking studies show strong binding of FHD to BSA (BSA, PDB ID: 6QS9), with a binding energy comparable to the anti-inflammatory drug diclofenac (DIF). MD simulations demonstrate that the 6QS9-FHD complex exhibits superior stability over 100 ns, lower root RMSD, and consistent compactness compared to 6QS9-DIF. Radius of gyration (Rg) and solvent-accessible surface area (SASA) analyses further confirm the stability of the FHD complex. These findings suggest FHD's potential as a candidate for anti-inflammatory applications.

Keywords: N-ferrocenylmethyl-N-phenylbenzohydrazide; Molecular docking; MD simulations; BSA

1. INTRODUCTION

With the rise of computational tools, bioinformatics has become a reliable approach for accurately predicting the physicochemical and pharmacological characteristics of various compounds. This advancement is primarily driven by the growing field of in silico studies, which utilize computer-aided drug design software and integrated collaborative platforms [1].

This computational approach proves particularly valuable as a preliminary step before performing in vitro and in vivo experiments [2]. The integration of in silico techniques, including molecular docking, has significantly advanced various research areas, such as genetic and evolutionary biology [3]. These methods enable the prediction of molecular interactions with specific receptors at the atomic scale, relying on energy transfer mechanisms [4]. Such insights assist researchers in developing more efficient therapeutic strategies, particularly for combating inflammation.

Human health is continuously challenged by various agents, including microorganisms, chemicals, radiation, and physical factors, which can also cause detrimental effects at the genetic level [5,6]. However, the human body employs several natural defense mechanisms to preserve its physiological balance. Among these, inflammation serves as a critical immune response, primarily driven by immune cells that release key mediators like cytokines, chemokines, and interferons to facilitate tissue healing and recovery [7]. Nevertheless, under pathological conditions, immune system dysfunction may trigger an excessive inflammatory response, contributing to the onset of chronic diseases such as ulcers, asthma, tuberculosis, and rheumatoid arthritis [8].

Ferrocenylmethyl derivatives have gained considerable attention due to their remarkable stability under aqueous and aerobic conditions, as well as their diverse biological applications [9–16]. Extensive research has shown that specific ferrocene-based derivatives display potent activities against a wide range of diseases, including fungal and bacterial infections [17–21], cancer [22,23], diabetes [24], malaria [16,25], and inflammation [26].

In this context, we investigated the interaction of N-ferrocenylmethyl-N-phenylbenzohydrazide (FHD) with bovine serum albumin (BSA) using molecular docking studies. To further assess its molecular stability and behavior, molecular dynamics (MD) simulations were performed for a duration of 100 ns.

2. RESULTS AND DISCUSSION

2.1. Docking analysis

The docking protocol was assessed by reintroducing the co-crystallized ligand into the binding site of its respective protein, as outlined in the methodology. The results from the validation experiments indicated a good alignment between the docked conformation of the ligand and its original structure, with an RMSD value of 1.315 Å, Figure 1.

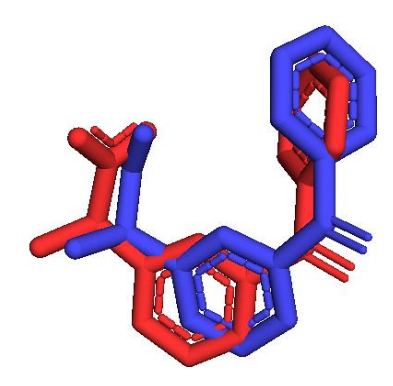


Fig.1. Structures of (Blue) native co-crystal and (Red) dock pose in the active site of 6QS9

As presented in Table 1, FHD exhibited a higher binding affinity to BSA with a binding free energy (ΔG) of -9.21 kcal/mol, compared to the standard anti-inflammatory drug diclofenac (DIF), which showed a ΔG of -7.79 kcal/mol.

Both FHD and DIF formed two hydrogen bonds with key amino acids in the active site, namely Tyrosine (TYR A:149) and Arginine (ARG A:256), as detailed in Table 1 and Figure 2.

DIF was further stabilized by five hydrophobic interactions involving Leucine (LEU A:218, LEU A:259), Alanine (ALA A:260), and Isoleucine (ILE A:263, ILE A:289).

FHD exhibited similar hydrophobic interactions with the amino acids as observed with DIF, including LEU A:218 (two bonds), LEU A:259, ALA A:260, and ILE A:289 (two bonds). In addition to other hydrophobic bonds with ARG A:198, ARG A:217, LYS A:221, PHE A:222, ARG A:256, and ALA A:290 (four bonds). Moreover, FHD also displayed one electrostatic interaction with ARG A:298, which contributed to its enhanced binding affinity and overall stability within the active site.

These findings highlight FHD's enhanced binding interactions compared to DIF, suggesting its potential as a candidate for anti-inflammatory applications.

Table 1. Interaction type, and Binding interaction of ligands with BSA receptors

Ligand	Binding	Residues	
	interaction	Residues	
	Conventional H-	TVD A.140 ADC A.256	
DIF	Bond	TYR A:149, ARG A:256	
	Pi-Sigma	LEU A:218, ILE A:289	
	Pi-Alkyl	LEU A:259, ALA A:260, ILE A:263	
	Conventional H-	TYR A:149, ARG A:256	
	Bond	1 1 K A.149, ARG A.230	
	Electrostatic	ARG A:198	
EHD	Pi-Sigma	ALA A:290	
FHD	Alkyl	ARG A:217, LEU A:218, LYS A:221,	
		ILE A:289, ALA A:290	
	Pi-Alkyl	PHE A:222, ARG A:256, LEU A:259,	
		ALA A:260, ILE A:289, ALA A:290	

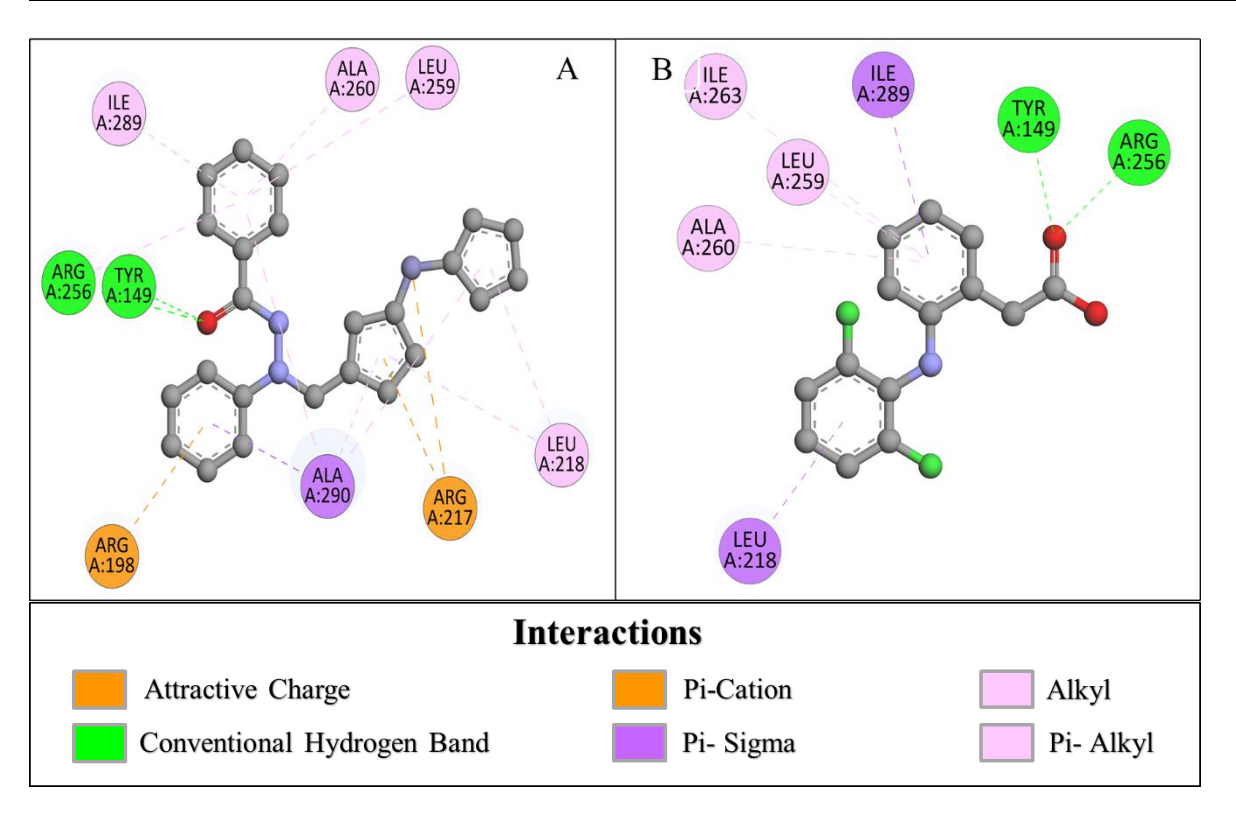


Fig.2. 2D illustration of possible interactions of FHD and DIF with 6QS9 protein

2.2. DFT calculations studies

2.2.1. FMO and MEP surface

The HOMO-LUMO energy gap ($\Delta E = E_{LUMO} - E_{HOMO}$) provides valuable insights into a compound's reactivity, with HOMO acting as the electron donor and LUMO as the electron acceptor [27–30]. The MEP surface helps identify reactive regions by showing the distribution of electronic charges. Blue regions indicate electron-deficient areas, making them favorable for nucleophilic attack, while red regions, being electron-rich, are suited for electrophilic attack [27–30]. The HOMO-LUMO energy and MEP surfaces of the FHD compound are shown in Figure 3. The HOMO is mainly concentrated on the ferrocene moiety, whereas the LUMO is predominantly associated with the benzo hydrazide group. The energy gap indicates the presence of intramolecular charge transfer interactions [31,32]. Smaller ΔE values suggest greater charge transfer, while larger energy gaps are linked to increased stability and reduced reactivity [33,34]. As depicted in Figure 3, the HOMO and LUMO energies for FHD are -5.586 eV and -1.588 eV, respectively, resulting in an ΔE_{L-H} of 3.998 eV. The most negative electrostatic potential is found around the oxygen atom of the carbonyl group (C=O) and the aniline ring, while the positive regions are centered on the hydrogen atoms of the amine group (NH), as well as the hydrogen atoms of the ferrocene moiety and benzo hydrazide ring.

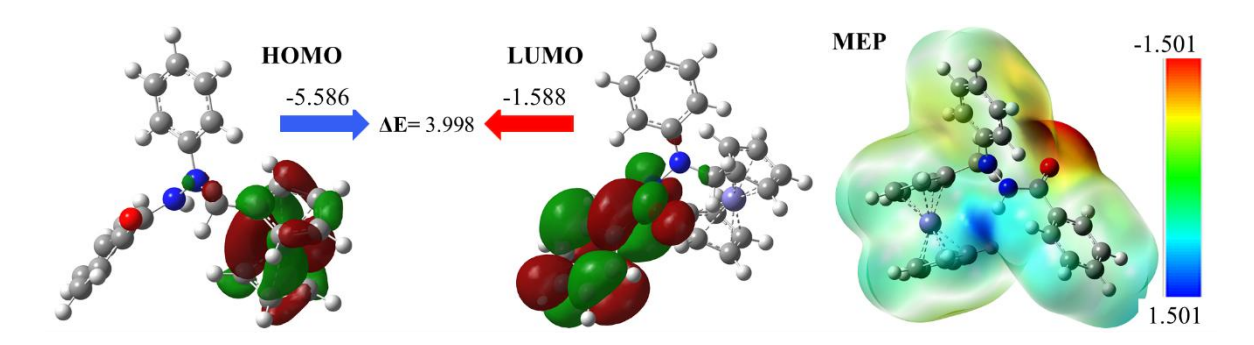


Fig.3. HOMO-LUMO and MEP surfaces of FHD

2.2.2. RDG Analysis

The stability of the FHD was largely due to weak intermolecular and intramolecular interactions, analyzed using the reduced density gradient (RDG) method, focusing on non-covalent forces (NCI). The $\lambda 2$ sign differentiate between bound ($\lambda 2 < 0$) and unbound ($\lambda 2 > 0$) interactions. Red peaks indicate steric repulsion within the ring structure, green peaks corresponded to Van der

Waals interactions, and blue spikes represented electrostatic forces, such as hydrogen and halogen bonding [35,36].

The 2D and 3D RDG plots (Figure 4) reveal that steric effects, represented by red color, were observed within the range of 0.01 a.u. to 0.05 a.u., particularly at the centers of the phenyl rings, cyclopentadiene rings, and around the ferrocene atom. Van der Waals interactions are indicated by red-green mixed spikes, found in the range of -0.015 a.u. to 0.01 a.u., particularly between the hydrogen atoms and the carbonyl (C=O) group or the carbon atoms in the phenyl ring.

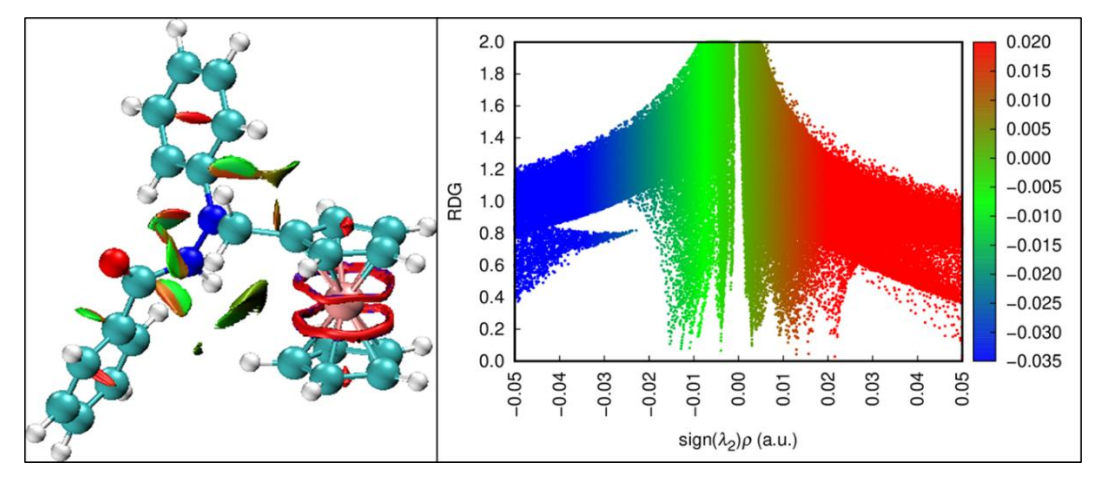


Fig.4. RDG (right) and NCI (left) plot of FHD

2.3. MD Simulations

The stability of the molecular configurations throughout a 100 ns MD simulation was evaluated using RMSD, RMSF. RG and SASA analysis (Table 2, Figure 4).

Table 2. The average value obtained from molecular dynamics simulations for FHD and DIF

Metrics	6QS9-	6QS9-
	FHD	DIF
RMSD	0.141	0.411
(nm)		
RMSF	0.175	0.166
(nm)		
Rg (nm)	2.741	2.715
SASA	292.24	290.53
(nm2)		

As shown in Figure 5, the initial analysis of RMSD values indicates that the 6QS9-FHD complex maintains significant conformational stability within the protein's active site, with an average RMSD of 0.141 nm. This stability is evident as the RMSD remains constant throughout the simulation period. In contrast, the standard drug diclofenac (6QS9-DIF) shows a higher average RMSD of 0.411 nm over 100 ns. After an initial increase to 0.510 nm by 22 ns, the RMSD remains stable for the remainder of the simulation.

The RMSF analysis highlights the flexibility and mobility of individual amino acid residues in the 6QS9-FHD and 6QS9-DIF complexes (Figure 5). The average RMSF value for the 6QS9-FHD complex was found to be 0.175 nm, which is comparable to the 6QS9-DIF complex (0.166 nm), indicating lower flexibility in both complexes.

The Rg was analyzed to evaluate the compactness and molecular stability of the docked complexes, while SASA analysis was performed to examine ligand-induced changes in the solvent-accessible surface area. Both the FHD and DIF complexes exhibited comparable Rg and SASA fluctuations. The Rg values were 2.741 nm for 6QS9-FHD and 2.715 nm for 6QS9-DIF. Similarly, the average SASA values were 292.24 nm² and 290.53 nm² for 6QS9-FHD and 6QS9-DIF, respectively.

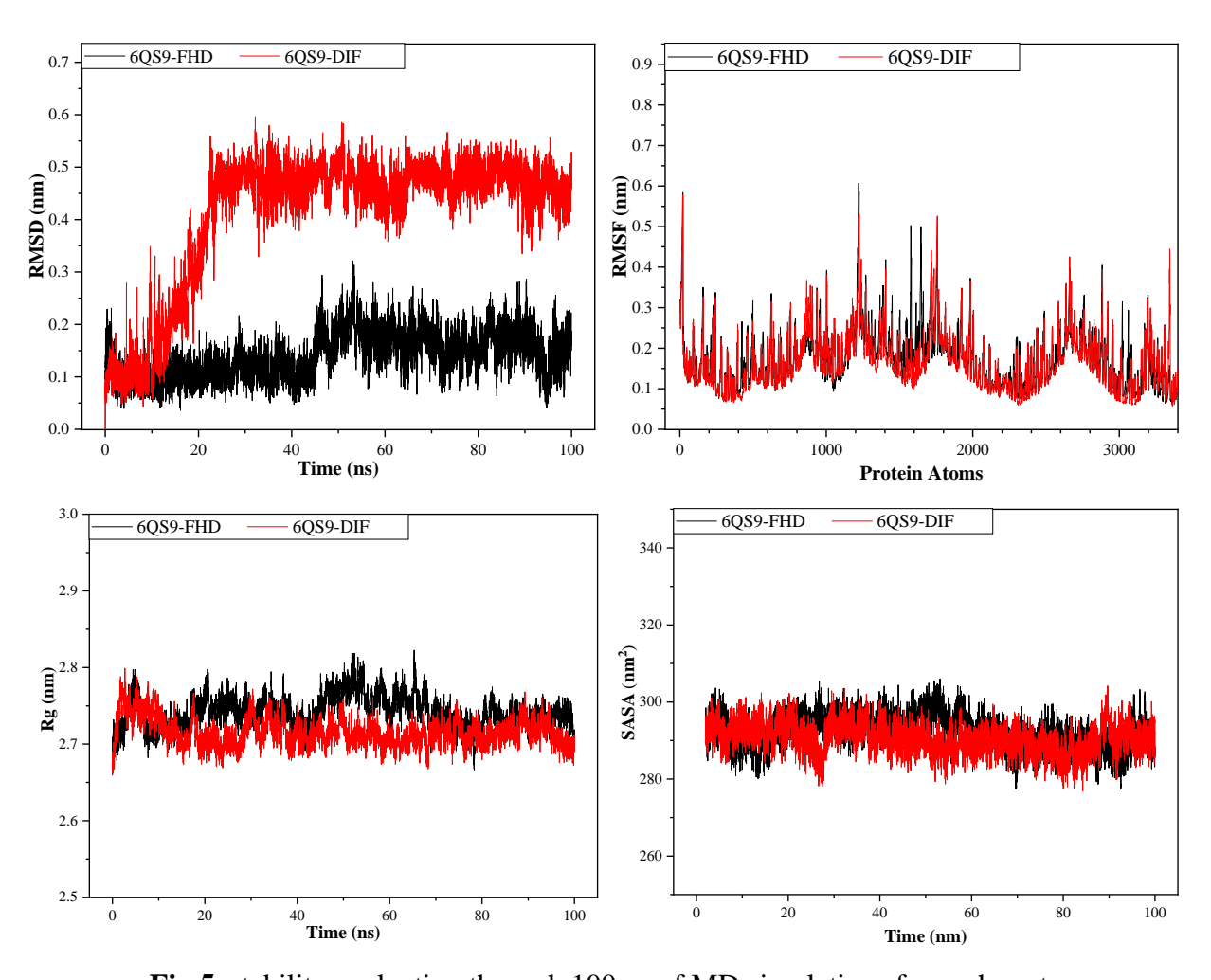


Fig.5. stability evaluation through 100 ns of MD simulations for each system

2.4. Theoretical methodology

2.4.1. Computational details

The structural optimization of FHD was carried out using Gaussian 16 W software [37], applying the DFT method at the B3LYP/6-311++G (d,p) level of theory [38]. Essential parameters, including the energy of the highest occupied molecular orbital (E_{HOMO}), the energy of the lowest unoccupied molecular orbital (E_{LUMO}), the energy gap (ΔE) between HOMO and LUMO, molecular electrostatic potential (MEP) and reduced density gradient (RDG) were calculated.

2.4.2. Docking studies:

The crystallographic structure of the target protein BSA (PDB ID: 6QS9) was retrieved from the RCSB PDB database [39]. Preprocessing was carried out using AutoDock Tools 1.5.7 (ADT) software [40], where water molecules and heteroatoms were removed. Additionally, Kollman and

Gasteiger charges, along with polar hydrogens, were added to the protein to prepare it for docking simulations.

The geometry of FHD was derived from its DFT-optimized structure and saved in PDB format. The 3D structure of the reference drug diclofenac (DIF) was acquired from PubChem [41], and MMFF charges were assigned using ADT.

Key amino acids in the active site were identified with Discovery Studio Visualizer (DSV) software [42] based on the co-crystallized ligand. Docking simulations were performed within a grid box of dimensions $50 \times 50 \times 50$ Å (xyz points), with a grid spacing of 0.375 Å. The grid center coordinates were set to X = -11.134, Y = -8.424, and Z = 14.203.

The docking protocol's validity was verified by re-docking the co-crystallized ligand into its protein's binding site. According to the literature [43], docking results are considered reliable if the root mean square deviation (RMSD) value is below 2.0 Å compared to the experimental structure. Docking calculations were performed using Lamarckian genetic algorithms, with each experiment consisting of 20 runs. These runs produced various ligand binding energies and corresponding conformations. The conformation with the lowest binding energy was identified as the optimal pose and used for further docking analysis [44–48].

2.4.3. Molecular dynamics (MD) simulations:

The stability of biomolecular complexes was evaluated using 100 ns MD simulations with Gromacs-2023 on a GPU system [49]. The initial conformation was taken from the docked complex. Protein topologies were generated with the AMBERGS force field, and ligand parameters were assigned using the general AMBER force field (GAFF).

The systems were solvated in a TIP3P water cubic box, neutralized with Na+ and Cl- ions, and energy-minimized using steepest descent and conjugate gradient methods until forces dropped below 10.0 kJ/mol. NVT equilibration was conducted at 300 K for 0.1 ns using the v-rescale thermostat, followed by 0.1 ns NPT equilibration with Berendsen pressure coupling [50,51].

To explore the biomolecular behavior of FHD compound within target protein active sites and its impact on essential biological functions, several key parameters were analyzed. The root mean square deviation (RMSD) was used to monitor changes in the backbone atoms of target proteins, while root mean square fluctuation (RMSF) quantified the flexibility of individual amino acids. The radius of gyration (Rg) was calculated to evaluate the compactness of the complexes, and the

solvent-accessible surface area (SASA) was determined to assess the overall stability of the systems.

3. CONCLUSION

The computational evaluation of ferrocenylmethyl-N-phenylbenzohydrazide (FHD) binding to bovine serum albumin (BSA) demonstrated its strong binding affinity, as confirmed by molecular docking. DFT calculations, including FMO, MEP, and RDG analyses, established the electronic and structural features of FHD, highlighting its molecular stability and regions prone to interactions. Comparative studies with diclofenac (DIF), an anti-inflammatory drug, revealed that the 6QS9-FHD complex exhibited greater conformational stability and reduced fluctuations during MD simulations. Additionally, the Rg and SASA analyses indicated that FHD induces minimal structural perturbations in the protein. suggest FHD as a promising anti-inflammatory agent, warranting further in vitro and in vivo studies.

4. ACKNOWLEDGMENTS

This work was supported by the directorate-general of scientific research and technological development (DGRSDT) and the laboratory of valorization and technology of Saharan resources (VTRS) (project code: B00L01UN390120150001).

5. REFERENCES

- [1] M. Zloh, S.B. Kirton, The Benefits of In Silico Modeling to Identify Possible Small-Molecule Drugs and Their Off-Target Interactions, Future Med Chem 10 (**2018**) 423–432. https://doi.org/10.4155/fmc-2017-0151.
- [2] S. Tian, J. Wang, Y. Li, D. Li, L. Xu, T. Hou, The application of in silico drug-likeness predictions in pharmaceutical research, Adv Drug Deliv Rev 86 (**2015**) 2–10. https://doi.org/10.1016/j.addr.2015.01.009.
- [3] A. Villalobos, M. Welch, J. Minshull, In Silico Design of Functional DNA Constructs, in: **2012**: pp. 197–213. https://doi.org/10.1007/978-1-61779-564-0_15.
- [4] V.L. Maruthanila, R. Elancheran, N.K. Roy, A. Bhattacharya, A.B. Kunnumakkara, S. Kabilan, J. Kotoky, In silico Molecular Modelling of Selected Natural Ligands and their Binding

- Features with Estrogen Receptor Alpha, Curr Comput Aided Drug Des 15 (**2018**) 89–96. https://doi.org/10.2174/1573409914666181008165356.
- [5] F.O. Vannberg, S.J. Chapman, A.V.S. Hill, Human genetic susceptibility to intracellular pathogens, Immunol Rev 240 (**2011**) 105–116. https://doi.org/10.1111/j.1600-065X.2010.00996.x.
- [6] E. Janik, M. Ceremuga, M. Niemcewicz, M. Bijak, Dangerous Pathogens as a Potential Problem for Public Health, Medicina (B Aires) 56 (**2020**) 591. https://doi.org/10.3390/medicina56110591.
- [7] C.A. Dinarello, Proinflammatory Cytokines, Chest 118 (**2000**) 503–508. https://doi.org/10.1378/chest.118.2.503.
- [8] R.H. Straub, C. Schradin, Chronic inflammatory systemic diseases an evolutionary trade-off between acutely beneficial but chronically harmful programs, Evol Med Public Health (**2016**) eow001. https://doi.org/10.1093/emph/eow001.
- [9] X.-F. Huang, L.-Z. Wang, L. Tang, Y.-X. Lu, F. Wang, G.-Q. Song, B.-F. Ruan, Synthesis, characterization and antitumor activity of novel ferrocene derivatives containing pyrazolyl-moiety, J Organomet Chem 749 (**2014**) 157–162. https://doi.org/10.1016/j.jorganchem.2013.08.043.
- [10] J.-N. Wei, Z.-D. Jia, Y.-Q. Zhou, P.-H. Chen, B. Li, N. Zhang, X.-Q. Hao, Y. Xu, B. Zhang, Synthesis, characterization and antitumor activity of novel ferrocene-coumarin conjugates, J Organomet Chem 902 (**2019**) 120968. https://doi.org/10.1016/j.jorganchem.2019.120968.
- [11] B. Lal, A. Badshah, A.A. Altaf, M.N. Tahir, S. Ullah, F. Huq, Synthesis, characterization and antitumor activity of new ferrocene incorporated N,N'-disubstituted thioureas, Dalton Transactions 41 (2012) 14643–14650. https://doi.org/10.1039/c2dt31570j.
- [12] B. Lal, A. Badshah, A.A. Altaf, N. Khan, S. Ullah, Miscellaneous applications of ferrocene-based peptides/amides, Appl Organomet Chem 25 (**2011**) 843–855. https://doi.org/10.1002/aoc.1843.
- [13] F. Asghar, A. Badshah, B. Lal, S. Zubair, S. Fatima, I.S. Butler, Facile synthesis of fluoro, methoxy, and methyl substituted ferrocene-based urea complexes as potential therapeutic agents, Bioorg Chem 72 (**2017**) 215–227. https://doi.org/10.1016/j.bioorg.2017.04.016.
- [14] J.C. Swarts, E.W. Neuse, G.J. Lamprecht, Synthesis and characterization of water-soluble polyaspartamide-ferrocene conjugates for biomedical applications, Journal of Inorganic and Organometallic Polymers 4 (**1994**) 143–153. https://doi.org/10.1007/BF01036539.

- [15] D.R. van Staveren, N. Metzler-Nolte, Bioorganometallic Chemistry of Ferrocene, Chem Rev 104 (**2004**) 5931–5986. https://doi.org/10.1021/cr0101510.
- [16] T. Itoh, S. Shirakami, N. Ishida, Y. Yamashita, T. Yoshida, H.S. Kim, Y. Wataya, Synthesis of novel ferrocenyl sugars and their antimalarial activities., Bioorg Med Chem Lett 10 (**2000**) 1657–9. https://doi.org/10.1016/s0960-894x(00)00313-9.
- [17] S. Benabdesselam, H. Izza, T. Lanez, E.K. Guechi, Synthesis, antioxidant and antibacterial activities of 3-nitrophenyl ferrocene, IOP Conf Ser Mater Sci Eng 323 (**2018**) 012007. https://doi.org/10.1088/1757-899X/323/1/012007.
- [18] C. Biot, N. François, L. Maciejewski, J. Brocard, D. Poulain, Synthesis and antifungal activity of a ferrocene-fluconazole analogue., Bioorg Med Chem Lett 10 (**2000**) 839–41. https://doi.org/10.1016/s0960-894x(00)00120-7.
- [19] B. Long, C. He, Y. Yang, J. Xiang, Synthesis, characterization and antibacterial activities of some new ferrocene-containing penems, Eur J Med Chem 45 (**2010**) 1181–1188. https://doi.org/10.1016/j.ejmech.2009.12.045.
- [20] S. Ali, A.A. Altaf, A. Badshah, Imtiaz-Ud-Din, B. Lal, S. Kamal, S. Ullah, DNA interaction, antibacterial and antifungal studies of 3-nitrophenylferrocene, Journal of the Chemical Society of Pakistan 35 (**2013**) 922–928.
- [21] E.M. Njogu, B. Omondi, V.O. Nyamori, Synthesis, physical and antimicrobial studies of ferrocenyl-N-(pyridinylmethylene)anilines and ferrocenyl-N-(pyridinylmethyl)anilines, South African Journal of Chemistry 69 (**2016**) 51–66. https://doi.org/10.17159/0379-4350/2016/v69a7.
- [22] A. Adaika, A. Adaika, T. Lanez, E. Lanez, in Vitro and in Silico Evaluation of Anticancer Activity of N,N-Dimethylaminomethylferrocene, Journal of Fundamental and Applied Sciences 11 (2019) 748–768. https://doi.org/10.4314/JFAS.V11I2.14.
- [23] L. Tabrizi, T.L.A. Nguyen, H.D.T. Tran, M.Q. Pham, D.Q. Dao, Antioxidant and Anticancer Properties of Functionalized Ferrocene with Hydroxycinnamate Derivatives—An Integrated Experimental and Theoretical Study, J Chem Inf Model 60 (2020) 6185–6203. https://doi.org/10.1021/acs.jcim.0c00730.
- [24] S. Bano, A. Khan, F. Asghar, M. Usman, A. Badshah, S. Ali, Computational and Pharmacological Evaluation of Ferrocene-Based Acyl Ureas and Homoleptic Cadmium Carboxylate Derivatives for Anti-diabetic Potential, Front Pharmacol 8 (2018) 1–16. https://doi.org/10.3389/fphar.2017.01001.

- [25] O. Domarle, G. Blampain, H. Agnaniet, T. Nzadiyabi, J. Lebibi, J. Brocard, L. Maciejewski, C. Biot, A.J. Georges, P. Millet, In Vitro Antimalarial Activity of a New Organometallic Analog, Ferrocene-Chloroquine, Antimicrob Agents Chemother 42 (1998) 540–544. https://doi.org/10.1128/AAC.42.3.540.
- [26] W.-Y. Guo, L.-Z. Chen, B.-N. Shen, X.-H. Liu, G.-P. Tai, Q.-S. Li, L. Gao, B.-F. Ruan, Synthesis and in vitro and in vivo anti-inflammatory activity of novel 4-ferrocenylchroman-2-one derivatives, J Enzyme Inhib Med Chem 34 (2019) 1678–1689. https://doi.org/10.1080/14756366.2019.1664499.
- [27] M. Milusheva, M. Todorova, V. Gledacheva, I. Stefanova, M. Feizi-Dehnayebi, M. Pencheva, P. Nedialkov, Y. Tumbarski, V. Yanakieva, S. Tsoneva, Novel anthranilic acid hybrids—An alternative weapon against inflammatory diseases, Pharmaceuticals 16 (2023) 1660.
- [28] A.S. Dorafshan Tabatabai, E. Dehghanian, H. Mansouri-Torshizi, M. Feizi-Dehnayebi, Computational and experimental examinations of new antitumor palladium (II) complex: CT-DNA-/BSA-binding, in-silico prediction, DFT perspective, docking, molecular dynamics simulation and ONIOM, J Biomol Struct Dyn 42 (2024) 5447–5469.
- [29] L. Messaadia, Y. Bekkar, M. Benamira, H. Lahmar, Predicting the antioxidant activity of some flavonoids of Arbutus plant: A theoretical approach, Chemical Physics Impact 1 (**2020**) 100007. https://doi.org/10.1016/j.chphi.2020.100007.
- [30] R. Bendaas, Y. Bekkar, L. Messaadia, L. Bourougaa, A. Messaoudi, S. Kiamouche, B. Messaoud, Computational-based investigation of antioxidative potential polyphenolic compounds of Salvia officinalis L.: combined DFT and molecular docking approaches, J Mol Model 30 (2024) 87. https://doi.org/10.1007/s00894-024-05866-8.
- [31] K. Karrouchi, S.A. Brandán, Y. Sert, H. El-Marzouqi, S. Radi, M. Ferbinteanu, M.E.A. Faouzi, Y. Garcia, Synthesis, X-ray structure, vibrational spectroscopy, DFT, biological evaluation and molecular docking studies of (E)-N'-(4-(dimethylamino) benzylidene)-5-methyl-1H-pyrazole-3-carbohydrazide, J Mol Struct 1219 (**2020**) 128541.
- [32] I.M. Khan, A. Khan, S. Shakya, M. Islam, Exploring the photocatalytic activity of synthesized hydrogen bonded charge transfer co-crystal of chloranilic acid with 2-ethylimidazole: DFT, molecular docking and spectrophotometric studies in different solvents, J Mol Struct 1277 (2023) 134862.

- [33] M. Alizadeh, Z. Mirjafary, H. Saeidian, Straightforward synthesis, spectroscopic characterizations and comprehensive DFT calculations of novel 1-ester 4-sulfonamide-1, 2, 3-triazole scaffolds, J Mol Struct 1203 (**2020**) 127405.
- [34] M.N. Tahir, K.S. Munawar, M. Feizi-Dehnayebi, M. Ashfaq, M.E. Muhammed, One-dimensional polymer of copper with salicylic acid and pyridine linkers: Synthesis, characterizations, solid state assembly investigation by hirshfeld surface analysis, and computational studies, J Mol Struct 1297 (2024) 136956.
- [35] F. Akman, A. Demirpolat, A.S. Kazachenko, A.S. Kazachenko, N. Issaoui, O. Al-Dossary, Molecular Structure, Electronic Properties, Reactivity (ELF, LOL, and Fukui), and NCI-RDG Studies of the Binary Mixture of Water and Essential Oil of Phlomis bruguieri, Molecules 28 (2023) 2684. https://doi.org/10.3390/molecules28062684.
- [36] S. Khan, H. Sajid, K. Ayub, T. Mahmood, Adsorption behaviour of chronic blistering agents on graphdiyne; excellent correlation among SAPT, reduced density gradient (RDG) and QTAIM analyses, J Mol Liq 316 (2020) 113860. https://doi.org/10.1016/j.molliq.2020.113860.
- [37] E.U.A.-R.-S.R.P. Frisch, M.J., Trucks, G.W., Schlegel, H.B., Scuseria, G.E., Robb, M.A., Cheeseman, J.R.; Scalmani, G.; Barone, V.; Petersson, G.A.; Nakatsuji, H.; Li, X.; Caricato, M.; Marenich, A.V.; Bloino, J., Janesko, B.G., Gomperts, R., Mennucci, B., Hratchian, H.P., Gaussian 16, Revision B.01, (2016) Gaussian 16, Revision A.03, Gaussian, Inc., Wallin.
- [38] A.D. Becke, Density-functional thermochemistry. III. The role of exact exchange, J Chem Phys 98 (1993) 5648–5652. https://doi.org/10.1063/1.464913.
- [39] H.M. Berman, The Protein Data Bank, Nucleic Acids Res 28 (**2000**) 235–242. https://doi.org/10.1093/nar/28.1.235.
- [40] G.M. Morris, R. Huey, W. Lindstrom, M.F. Sanner, R.K. Belew, D.S. Goodsell, A.J. Olson, AutoDock4 and AutoDockTools4: Automated docking with selective receptor flexibility, J Comput Chem 30 (2009) 2785–2791. https://doi.org/10.1002/jcc.21256.
- [41] S. Kim, J. Chen, T. Cheng, A. Gindulyte, J. He, S. He, Q. Li, B.A. Shoemaker, P.A. Thiessen, B. Yu, L. Zaslavsky, J. Zhang, E.E. Bolton, PubChem 2023 update, Nucleic Acids Res 51 (2023) D1373–D1380. https://doi.org/10.1093/nar/gkac956.
- [42] D.S. BIOVIA, Discovery studio visualizer, 2020, Dassault Systèmes, San Diego (**2020**)., (n.d.).

- [43] R. Wang, Y. Lu, S. Wang, Comparative Evaluation of 11 Scoring Functions for Molecular Docking, J Med Chem 46 (**2003**) 2287–2303. https://doi.org/10.1021/jm0203783.
- [44] A. Sagaama, O. Noureddine, S.A. Brandán, A.J. Jędryka, H.T. Flakus, H. Ghalla, N. Issaoui, Molecular docking studies, structural and spectroscopic properties of monomeric and dimeric species of benzofuran-carboxylic acids derivatives: DFT calculations and biological activities, Comput Biol Chem 87 (2020) 107311. https://doi.org/10.1016/j.compbiolchem.2020.107311.
- [45] T. Ben Issa, A. Sagaama, N. Issaoui, Computational study of 3-thiophene acetic acid: Molecular docking, electronic and intermolecular interactions investigations, Comput Biol Chem 86 (2020) 107268. https://doi.org/10.1016/j.compbiolchem.2020.107268.
- [46] S. Ramalakshmi, K. Sonanki, R. Prakash, G. Usha, K. Karpagalakshmi, E.R. Nagarajan, N. Selvapalam, In-silico approach of effect of protein on complexation of cucurbit[7]uril with N-(ferrocenylmethyl) aniline, Mater Today Proc 51 (**2021**) 1733–1737. https://doi.org/10.1016/j.matpr.2020.11.720.
- [47] B. Kurt, H. Temel, M. Atlan, S. Kaya, Synthesis, characterization, DNA interaction and docking studies of novel Schiff base ligand derived from 2,6-diaminopyridine and its complexes, J Mol Struct 1209 (**2020**) 127928. https://doi.org/10.1016/j.molstruc.2020.127928.
- [48] A. Arunadevi, N. Raman, Indole-derived water-soluble N, O bi-dentate ligand-based mononuclear transition metal complexes: in silico and in vitro biological screening, molecular docking and macromolecule interaction studies, J Biomol Struct Dyn 38 (**2020**) 1499–1513. https://doi.org/10.1080/07391102.2019.1611475.
- [49] D. Van Der Spoel, E. Lindahl, B. Hess, G. Groenhof, A.E. Mark, H.J.C. Berendsen, GROMACS: Fast, flexible, and free, J Comput Chem 26 (2005) 1701–1718. https://doi.org/10.1002/jcc.20291.
- [50] B. Lotfi, O. Mebarka, S.U. Khan, T.T. Htar, Pharmacophore-based virtual screening, molecular docking and molecular dynamics studies for the discovery of novel neuraminidase inhibitors, J Biomol Struct Dyn 42 (2024) 5308–5320. https://doi.org/10.1080/07391102.2023.2225007.
- [51] K. Anbarasu, S. Jayanthi, Identification of curcumin derivatives as human LMTK3 inhibitors for breast cancer: a docking, dynamics, and MM/PBSA approach, 3 Biotech 8 (**2018**) 228. https://doi.org/10.1007/s13205-018-1239-6.